Proceedings Paper:
Miyauchi, G., Talamali, M.S. and Gross, R. (2024) A comparative study of energy replenishment strategies for robot swarms. In: Hamann, H., Dorigo, M., Cáceres, L.P., Reina, A., Kuckling, J, Kaiser, T.K., Soorati, M., Hasselmann, K. and Buss, E., (eds.) Swarm Intelligence: 14th International Conference, ANTS 2024, Konstanz, Germany, October 9–11, 2024, Proceedings. International Conference on Swarm Intelligence (ANTS 2024), 09-11 Oct 2024, Konstanz, Germany. Lecture Notes in Computer Science, LNCS 14987. Springer, pp. 3-15. ISBN: 9783031709319. ISSN: 0302-9743. EISSN: 1611-3349.

https://doi.org/10.1007/978-3-031-70932-6_1

A Comparative Study of Energy Replenishment Strategies for Robot Swarms

Genki Miyauchi[1] [0000−0002−3349−6765], Mohamed S. Talamali[1] [0000−0002−2071−4030], and Roderich Groß[1,2] [0000−0003−1826−1375]

[1] Department of Automatic Control and Systems Engineering, The University of Sheffield, Sheffield, United Kingdom
{g.miyauchi,m.s.talamali}@sheffield.ac.uk
[2] Department of Computer Science, Technical University of Darmstadt, Darmstadt, Germany
roderich.gross@tu-darmstadt.de

Abstract. To enable long-term operations of swarms of energy-constrained robots, they need to manage both their in-flow and out-flow of energy. We consider two strategies for doing so: In the first strategy, all robots work at a remote location but due to their limited storage capacity must return to charge. In the second strategy, dedicated mobile chargers with finite storage capacity deliver energy to the remote location, substantially shortening the worker robots' commute. We compare the work performed and the energy efficiency of these strategies using physics-based simulations and reveal conditions under which their performance is close to theoretically derived upper bounds. We assess several factors, including the number of mobile chargers, their storage capacity, transfer losses, and the ratio of energy expended while working and travelling. Our findings confirm that mobile chargers can help increase the work performed, and even overall energy efficiency provided that their energy storage is larger than that of workers.

1 Introduction

When playing their part in real-world applications, swarms of robots will have to operate autonomously over extended periods of time. Examples include applications in environmental monitoring, surveillance, agriculture, construction, and mining [7,13,21]. In this context, energy is a key consideration, and both its in-flow (i.e. how a swarm replenishes its energy) and out-flow (i.e. how a swarm invests its energy) need careful consideration. At every moment of time, the robots ultimately devote some of their energy towards performing work versus securing energy to replenish.

Several studies consider swarms where the individual robots alternate between performing work and visiting charging points to replenish their finite energy storage [1,2,16,19,22]. To reduce charging times, stations offering robots to hot-swap their batteries have been considered [18]. To reduce travel times, optimised placements of (mobile) charging stations have been considered [5].

Other studies consider swarms where energy is transferred among members of finite storage capacity, a process referred to as energy trophallaxis [4,8,12,20]. Such an approach can promote division of labour, enabling some individuals to focus on certain tasks [3], while also reducing congestion near a shared resource [15] (e.g. at the charging station). To reduce transfer times, prior work [17] proposed robots that exchange energy by swapping batteries. Recent multi-robot platforms such as Freebot [6] have demonstrated low transfer times using supercapacitors, achieving duty cycles of up to 98%. However, several factors including ineffective strategies for sharing energy across the swarm or high energy transfer loss may potentially hinder uptake of this technology.

In this paper, we compare two strategies for regulating the in-flow and outflow of energy of a swarm of robots that is required to perform work at a remote location for an extended period of time. The first strategy makes exclusive use of fixed charging points. Every robot alternates between performing work at the remote location and recharging back at the base. The second strategy introduces the use of mobile charging units of limited storage capacity, which deliver energy to the working robots and recharge back at the base. The remaining robots alternate between performing work and replenishing via energy transfer from nearby mobile chargers. We formally derive some upper bounds for the amount of work performed and energy efficiency. Through a series of physics-based simulations, we identify conditions in which either strategy becomes favourable, considering among others the cost of being idle, moving and working, as well as the ratio of storage capacity of mobile chargers versus workers.

The paper is organised as follows. Section 2 presents the problem formulation and strategy for energy replenishing using fixed charging points, and presents a formal analysis. Section 3 presents the problem formulation and strategy for energy replenishing using mobile chargers. Section 4 describes the implementation of the strategies. Section 5 presents the results. Section 6 concludes the paper.

2 Energy Replenishing Using Fixed Charging Stations

2.1 Problem Scenario

Consider the 2D environment illustrated in Fig. 1a. It comprises three regions: (i) a *base* region (green), (ii) a *commuter* region (white), and (iii) a *work* region (red).

The environment contains a population of n_w robots (green circles), known as *workers*. At each time step, each robot can choose whether to move or remain stationary. When within the work region, the robot can choose in addition to perform work. A working robot performs work at a rate of 1 unit per time step.

Each worker has the capacity to store a maximum of $c_{w,max}$ units of energy. Its energy consumption is as follows:

1. A worker that is neither moving nor working consumes $\nu_{w,min}$ units of energy per time step. This is to support its core operations.

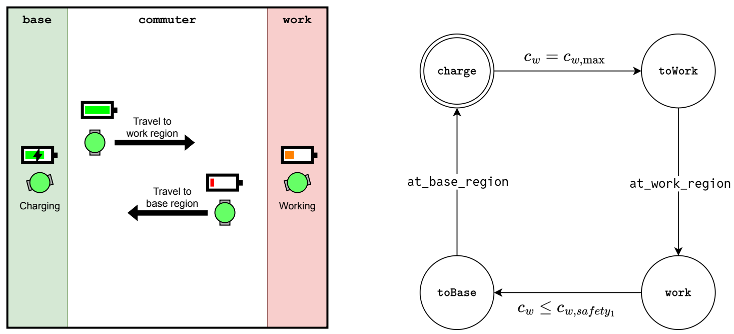

(a) (b)

Fig. 1. Energy replenishing using fixed charging stations. (a) The workers, represented by green disks, accumulate energy in the base region (green rectangle) before moving to the work region (red rectangle) to perform work. When a worker's energy storage runs low, it moves back to the base region to recharge. (b) Finite state machine executed by each robot.

2. A worker that is moving but not working consumes $\nu_{w,min} + \nu_{w,move}$ units of energy per time step.
3. A worker that is working but not moving consumes $\nu_{w,min} + \nu_{w,work}$ units of energy per time step.
4. A worker that is both moving and working consumes $\nu_{w,min} + \nu_{w,move} + \nu_{w,work}$ units of energy per time step.

While residing within the base region, a worker can accumulate (gross) energy at a rate of $\nu_{w,charge}$ units per time step. Its (net) accumulation of energy is $\nu_{w,charge} - \nu_{w,min}$ if stationary, and $\nu_{w,charge} - \nu_{w,min} - \nu_{w,move}$ otherwise. To reach the work region from the base region, the worker has to travel through the commuter region and vice versa.

We consider a mission over a finite duration τ. Initially, each worker's energy storage is assumed to be at full capacity. The workers' objective is to perform as many units of work as possible without any worker depleting their energy storage while outside the base region. As $\tau \to \infty$, theoretically, this allows the workers to keep operating autonomously for an indefinite period of time.

2.2 Strategy

Fig. 1b depicts a finite state machine that is executed by each worker. Initially, all workers are assumed to reside within the base region. Hence, at time zero, the worker is charging (state `charge`). Once its level of stored energy reaches full capacity, the worker travels towards the work region (state `toWork`). Once reaching it, the worker performs work (state `work`). Once the level of its stored energy is below some safety threshold, $c_{w,safety_1}$, the worker returns to the base region (state `toBase`).

2.3 Analysis

We formally derive an upper bound for the performance of workers. In this theoretical model, we assume that (i) there is no interference among the workers' bodies (i.e., the workers may move through each other); (ii) the base, commuter, and work regions are closed sets; (iii) all workers commute between the subsets of the boundary of the commuter region that are shared with the base region and work region, respectively, and (iv) the workers follow optimal trajectories.

At time 0, the worker leaves the base region at full capacity $c_{w,max}$. Let $\Delta_{w,commute}$ denote the time that it takes for the worker to reach the work region. At time $\Delta_{w,commute}$, the worker reaches the work region at capacity $c_{w,max} - (\nu_{w,min} + \nu_{w,move})\Delta_{w,commute}$, and chooses to perform work from this moment. Once having only $(\nu_{w,min} + \nu_{w,move})\Delta_{w,commute}$ units of energy left, the worker returns to the base region, arriving at the moment its energy storage reaches zero. It then charges its level of energy to full capacity, which takes $\Delta_{w,charge} = \frac{c_{w,max}}{\nu_{w,charge} - \nu_{w,min}}$ units of time. The cycle then repeats.

In every cycle, the time a worker performs work is given by

$$\Delta_{w,work} = \frac{c_{w,max} - 2(\nu_{w,min} + \nu_{w,move})\Delta_{w,commute}}{\nu_{w,min} + \nu_{w,work}}$$

The worker's duty cycle is the proportion of time it is working. It is given by

$$D_w = \frac{\Delta_{w,work}}{\Delta_{w,cycle}}$$

where $\Delta_{w,cycle} = \Delta_{w,work} + 2\Delta_{w,commute} + \Delta_{w,charge}$ is the duration of a worker's cycle.

The system's total amount of work performed is

$$W = n_w D_w \tau \tag{1}$$

We define the system's energy efficiency as the proportion of energy spent on performing work[3]:

$$E = 1 - \frac{(\nu_{w,min} + \nu_{w,move})2\Delta_{w,commute} + \nu_{w,min}(\Delta_{w,work} + \Delta_{w,charge})}{c_{w,max}} \tag{2}$$

$$= 1 - \Delta_{w,cycle}\frac{\nu_{w,min}}{c_{w,max}} - 2\Delta_{w,commute}\frac{\nu_{w,move}}{c_{w,max}} \tag{3}$$

3 Energy Replenishing Using Mobile Charging Stations

3.1 Problem Scenario

Consider the 2D environment illustrated in Fig. 2a. Compared to the scenario with fixed charging stations, we have a fourth region (blue) called *transfer* region, which sits in between the commuter and work regions.

[3] Note that devoting energy to core operations while performing work reduces a worker's efficiency.

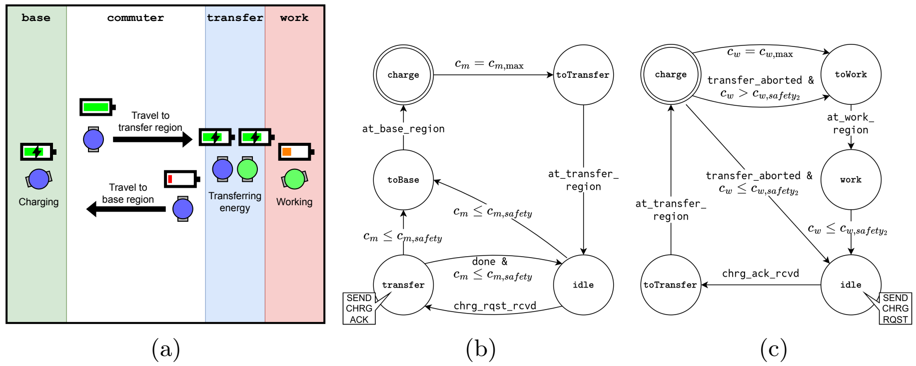

Fig. 2. Energy replenishing with mobile chargers of limited storage capacity. (a) Mobile chargers (represented as blue disks) transport energy from the base region to the transfer region (blue rectangle), where workers with low levels of energy arrive to recharge. (b) Finite state machine executed by each mobile charging unit. (c) Finite state machine executed by each working robot.

The environment contains n_w workers and n_m mobile chargers. The workers have the same capabilities as described earlier. The mobile chargers can move but are unable to perform any work.

Each mobile charger has the capacity to store a maximum of $c_{m,max}$ units of energy. Its energy consumption is as follows:

1. A mobile charger that is not moving consumes $\nu_{m,min}$ units of energy per time step. This is to support its core operations.
2. A mobile charger that is moving consumes $\nu_{m,min} + \nu_{m,move}$ units of energy per time step.

While residing within the base region, a mobile charger accumulates (gross) energy at a rate of $\nu_{m,charge}$ units per time step. Its (net) accumulation of energy is $\nu_{m,charge} - \nu_{m,min}$ if stationary, and $\nu_{m,charge} - \nu_{m,min} - \nu_{m,move}$ otherwise.

While residing within the transfer region, a mobile charger can agree to donate (gross) energy at a rate of $\nu_{m,transfer}$ units per time step to a worker in that region. The worker accumulates (gross) energy at a rate of $\xi\nu_{m,transfer}$ units per time step, where $\xi \in (0, 1]$ denotes the transfer loss. While energy is being transferred, both mobile charger and worker consume energy for their core operations, and, if applicable, their movement.

3.2 Strategy

Fig. 2b depicts a finite state machine that is executed by each mobile charger. Initially, all mobile chargers are assumed to reside within the base region. Hence, a mobile charger is charging at time zero (state `charge`). Once its level of stored energy reaches full capacity, the mobile charger travels towards the transfer region (state `toTransfer`). Once within the transfer region, the mobile charger pauses (state `idle`), waiting for a transfer request by a worker. If reaching a critical energy threshold, $c_{m,safety}$, the mobile charger travels back to the base region (state `toBase`). Otherwise, if a request is received, the mobile charger awaits the worker and upon arrival starts transferring energy (state `transfer`). The transfer is stopped as soon as the worker's storage is at full capacity, or the mobile charger's storage reaches a critical limit, $c_{m,safety}$. In the former case, the mobile charger transitions to state `idle`; in the latter case, it transitions to state `toBase`.

Fig. 2c depicts a finite state machine that is executed by each worker. Initially, all workers are assumed to reside within the base region. Hence, a worker is charging at time zero (state `charge`). Once its level of stored energy reaches full capacity, the worker moves towards the work region (state `toWork`). When within the work region, the worker performs work (state `work`). If the level of its stored energy gets below some safety threshold, $c_{w,safety_2}$, the worker suspends work (state `idle`) and (repetitively) requests an energy transfer. When its request gets acknowledged by a mobile charger, the worker approaches this charger (state `toTransfer`), and the transfer starts (state `charge`). Once its storage reaches full capacity, the worker moves towards the work region (state `toWork`). If the transfer is aborted prior to reaching full capacity, the worker probes whether the stored energy exceeds the safety threshold, $c_{w,safety_2}$. If it does, it moves towards the work region (state `toWork`). Otherwise, it seeks a transfer from a different mobile charger (state `idle`).

4 Implementation

To evaluate the energy replenishment strategies, we implement the state machines depicted in Figs. 1b, 2b and 2c on the e-puck [11] platform. The latter is a mobile differential-wheeled robot of diameter 7 cm and maximum speed $v_{\max} = 12\,\text{cm/s}$. We assume the robot is equipped with a range-and-bearing system enabling relative localisation and communication within a local neighbourhood of radius 0.533 m. All robots update their states using the state machines and use virtual forces to determine their direction of movement. Let $\mathbf{p}_{ij}$ denote robot j's position in the local coordinate system of robot i. The virtual force of robot i is given by

$$\mathbf{u}_i = \alpha\mathbf{u}_i^a + \beta\mathbf{u}_i^{rn} + \gamma\mathbf{u}_i^{ro}$$

where α, β and γ are positive scalars to weigh the influence of the components. Component $\mathbf{u}_i^a$ represents the attraction towards a goal, $\mathbf{g}_i$. It is defined as

$$\mathbf{u}_i^a = \frac{\mathbf{g}_i}{||\mathbf{g}_i||}\min(||\mathbf{g}_i||, v_{\max})$$

where goal $\mathbf{g}_i$ provides the position vector of a point in the base region, work region, or transfer region, respectively, where all vectors are defined relative to the position of robot i.

Component $\mathbf{u}_i^{rn}$ represents the repulsion from neighbouring robots. It is defined as

$$\mathbf{u}_i^{rn} = -\frac{1}{|\mathcal{N}_i|} \sum_{j \in N_i} \frac{\sigma^\lambda}{||\mathbf{p}_{ij}||^\lambda} \frac{\mathbf{p}_{ij}}{||\mathbf{p}_{ij}||}$$

where $\mathcal{N}_i$ denotes the set of robots in the neighbouring of robot i, σ is the desired separation between robots and λ is the exponent.

To avoid collisions with obstacles such as the walls, component $\mathbf{u}_i^{ro}$ uses the e-puck's eight proximity sensors which are distributed around the robot's circumference [11]. It is defined as

$$\mathbf{u}_i^{ro} = -\frac{1}{8d_{\max}} \sum_{j=1}^{8} (d_{\max} - d_j)\hat{\mathbf{v}}_j$$

where $d_{\max} = 10\,\mathrm{cm}$ is the range of the proximity sensors, d_j is the distance extracted from the j^{th} sensor and $\hat{\mathbf{v}}_j$ is the unit vector pointing from the robot's centre to the j^{th} sensor. Where sensor j detects no object, we set $d_j = d_{\max}$.

5 Results

We use physics-based simulations that consider collisions among robots to quantify the performance of the energy replenishment strategies in terms of both work performed and energy efficiency. Simulations are performed in ARGoS [14] with the physics and state machines updated every 0.1 s. The arena has a dimension (H×W) of 1.6 m×1.6 m and is bounded within $x, y \in [-0.8, 0.8]$. The base, work and transfer regions are each of dimension 0.3×1.6 m. We use $\alpha = 1$, $\beta = 100$, $\gamma = 1$, $\sigma = 0.1\,\mathrm{m}$ and $\lambda = 24$ for the robot's motion and no transfer loss ($\xi = 1$) per default. Trials are terminated after 10 minutes. Video recordings of the simulation can be found at [9]. The source code can be found at [10].

5.1 Fixed vs Mobile Charging Stations

For both strategies, an identical amount of workers is used, while for one strategy, mobile chargers are used as well. This is motivated by the observation that replacing a worker with a mobile charger does under no circumstances increase the amount of work being performed. On the contrary, it typically leads to a reduction[4]. Mobile chargers could nevertheless be useful as they are not required to perform any work and hence do not need potentially expensive work tools. They could be designed to move efficiently and offer increased energy storage.

We conduct trials with $n_w = 6$ workers. For the mobile charger strategy, we vary the number of chargers $n_m = \{1, 2, 4, 6, 8, 10, 12\}$ and their storage capacity $c_{m,max} = \phi c_{w,max}$ where $\phi = \{1, 1.5, 2, 4, 6\}$ to examine their effect on the aforementioned metrics.

[4] This is because the transfer of energy from mobile chargers to workers requires time, and during this time all parties consume a base level of energy.

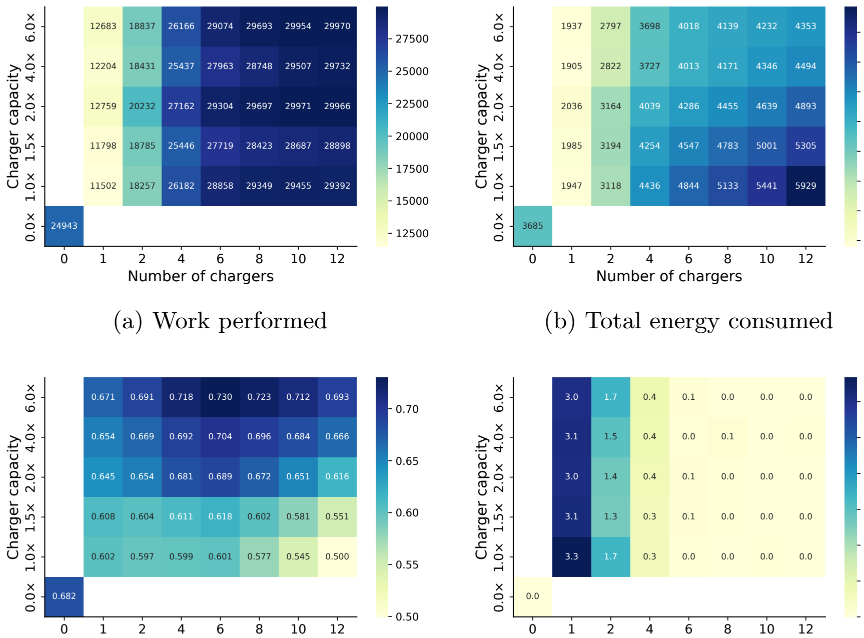

(a) Work performed

(b) Total energy consumed

(c) Energy efficiency

(d) Number of workers depleted

Fig. 3. The effect of the number of mobile chargers and their storage capacity on (a) the amount of work performed, (b) the total energy consumed, (c) the proportion of energy used to perform work, and (d) the number of depleted workers. The results of the static charger strategy are shown in 0 chargers and 0× charger capacity cells. Each configuration was tested for 50 trials.

Fig. 3a shows that 24943 units of work are performed if the workers charge at the base. This is 92.8% of the theoretical upper bound, obtained from equation (1), suggesting that the workers perform close to optimal in embodied simulations. When workers obtain their energy from mobile chargers, the amount of work performed increases with the number of mobile chargers, n_m, and plateaus after around $n_m = n_w$. The work performed with 6 and 12 mobile chargers, respectively, is 89.3% and 92.0% of what could optimally be achieved if the transfer region offered a constant supply of energy, which is equivalent to setting $\Delta_{w,commute} = 0$ in equation (1). Performing substantially more work would require additional workers.

Fig. 3b shows the total energy consumed by all robots, whereas Fig. 3c shows the energy efficiency, that is the proportion of total energy consumed that was devoted to performing work. Workers that charge at the base achieve an energy efficiency of 68.2%. This is only 12.6% less efficient than the upper bound obtained from equation (3). For workers obtaining energy from mobile chargers, the

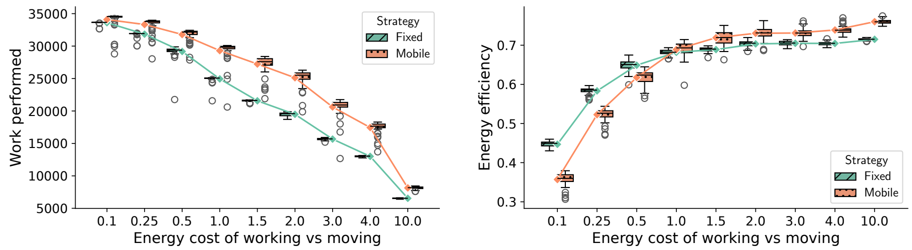

(a) (b)

Fig. 4. Comparison of the two strategies across different energy consumption ratios $\nu_{*,work}/\nu_{*,move}$. The solid lines connects the average values indicated by the diamond marker for each strategy. For *mobile* chargers, results are shown for 6 chargers and 2× charger capacity. (a) The amount of work performed and (b) the proportion of energy used to perform work. Each configuration was tested for 50 trials.

highest energy efficiency is consistently observed when $n_m = n_w$. This suggests that using fewer or additional mobile chargers would result in them or the workers wasting energy due to the time they spend waiting for each other. Moreover, deploying many mobile chargers with small capacity proves inefficient. Nevertheless, mobile chargers were able to help perform more work and even improve energy efficiency when their storage capacity was larger than the workers.

Fig. 3d reveals that a small amount of mobile chargers is unable to supply sufficient energy to all workers, even if being of high capacity. This is because each mobile charger can serve only a single robot at a time, which can cause in some robots depleting all their energy while waiting in the transfer region.

5.2 Impact of Workload

In the previous section, the rates of energy for performing work and for moving were assumed equal (i.e., $\nu_{*,move} = \nu_{*,work}$). Here, we investigate the impact of changing the energy rate required to perform work. We use $n_m = 6$ and $c_{m,max} = 2c_{w,max}$. This setting performed more work while maintaining a similar energy efficiency to the strategy without mobile chargers (see Fig. 3c).

Fig. 4a shows that as performing work becomes more energy-intense, less work is being performed. Furthermore, the strategy with mobile chargers outperforms the strategy without them. Fig. 4b shows that using mobile chargers results in higher energy efficiency when performing work that costs as much or more energy than moving. Otherwise, having workers return to the base for recharging is more energy-efficient.

5.3 Impact of Charging Rate

We explore the effect of the rate at which the agents charge and transfer energy. For the mobile charger strategy, we use $n_m = 6$ and $c_{m,max} = 2c_{w,max}$.

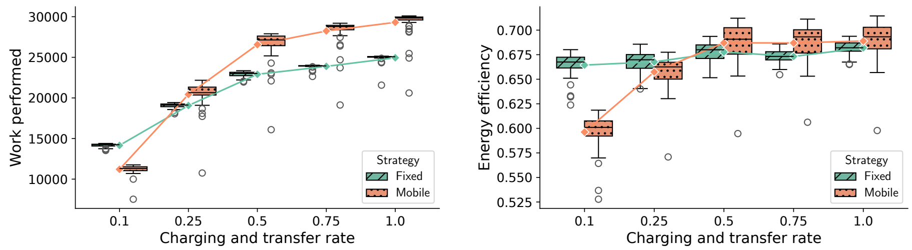

(a) (b)

Fig. 5. Comparison of the two strategies across different charging and transfer rates, $\nu_{*,charge} = \nu_{m,transfer}$. The solid lines connect the average values indicated by the diamond marker for each strategy. For *mobile* chargers, results are shown for 6 chargers and 2× charger capacity. (a) The amount of work performed and (b) the proportion of energy used to perform work. Each configuration was tested for 50 trials.

Fig. 5a shows that, for both strategies, the amount of work performed decreases as the charging and transfer rates, $\nu_{*,charge}$ and $\nu_{m,transfer}$, decreases. This is because robots need to spend a longer time to charge, reducing the time available for working.

Fig. 5b illustrates that the energy efficiency using fixed chargers remains fairly constant, presumably as movement dominates charging both in terms of duration and rate of energy consumption [see equation (3)]. In contrast, when using mobile chargers, the energy efficiency, while fairly constant at high values of $\nu_{*,charge}$, drops for $\nu_{*,charge} \leq 0.25$. As the charging times start to dominate, this disproportionately impacts the strategy with mobile chargers, as it requires twice the time for workers to charge.

5.4 Impact of Energy Transfer Loss

In this section, we introduce energy transfer loss, where a proportion of energy dissipates to the environment when mobile chargers transfer energy to workers. We examine $n_m = 6$ and $c_{m,max} = 2c_{w,max}$.

Fig. 6a reveals a non-monotonic dependency. The work performed first decreases as the transfer loss increases up to 40%, then increases at 50%, and finally decreases again from 60%. Upon close inspection of the simulation runs, it was observed that this was caused by the particular timings of the chargers and workers' activities. At a transfer loss of 50%, the mobile chargers could only transfer available energy to a single worker, and then had to return to the base. At a transfer loss of 40%, they attempted to transfer energy to a second worker, but had to abort the process prematurely to return to the base.

As expected, Fig. 6b shows that transfer loss negatively affects energy efficiency when using mobile chargers as some of the energy is lost while transferring energy to workers.

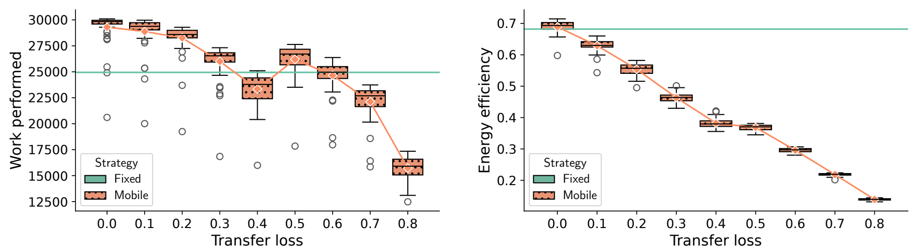

(a) (b)

Fig. 6. Comparison of the two strategies for different levels of transfer losses ξ. The solid line connects the average values indicated by the diamond marker for each strategy. For *mobile* chargers, results are shown for 6 chargers and 2× charger capacity. (a) The amount of work performed and (b) the proportion of energy used to perform work. Each configuration was tested for 50 trials.

6 Conclusion

This paper compared two energy replenishment strategies for a swarm of robots. In the first strategy, all robots were responsible for their energy and commuted between charging stations and remote locations of work. In the second strategy, robots capable of performing work at remote locations depended on the delivery and transfer of energy from mobile chargers. We compared the two strategies based on the amount of work performed and energy efficiency using physics-based simulations, and reveal conditions under which their performance is close to theoretically derived upper bounds. Results show that mobile chargers are beneficial when there is a sufficient, though not excessive, number of them and when they have a large energy capacity. Moreover, they are beneficial when more energy is required while performing work than while navigating. However, slow recharging rates as well as energy transfer losses negatively affect both the amount of work performed and energy efficiency.

Future work will investigate improved theoretical upper bounds for using mobile chargers and propose a hybrid strategy that allows robots to decide whether to wait for a mobile charger or travel back to the base region. We will also consider faster mobile chargers that are optimised for navigation, individual differences in battery health and validate our findings on a physical robotic platform.

Acknowledgments. This document is issued within the frame and for the purpose of the OpenSwarm project. This project has received funding from the European Union's Horizon Europe Framework Programme under Grant Agreement No. 101093046. Views and opinions expressed are however those of the author(s) only and the European Commission is not responsible for any use that may be made of the information it contains.

Disclosure of Interests. The authors declare no competing interests.

References

1. Chour, K., Reddinger, J.P., Dotterweich, J., Childers, M., Humann, J., Rathinam, S., Darbha, S.: An agent-based modeling framework for the multi-uav rendezvous recharging problem. Robotics and Autonomous Systems **166**, 104442 (2023)
2. Kannan, B., Marmol, V., Bourne, J., Dias, M.B.: The autonomous recharging problem: Formulation and a market-based solution. In: 2013 IEEE International Conference on Robotics and Automation. pp. 3503–3510. IEEE (2013)
3. Kreider, J.J., Janzen, T., Bernadou, A., Elsner, D., Kramer, B.H., Weissing, F.J.: Resource sharing is sufficient for the emergence of division of labour. Nature Communications **13**(1), 7232 (2022)
4. Kubo, M., Melhuish, C.: Robot trophallaxis: Managing energy autonomy in multiple robots. Proceedings of Towards Autonomous Robotic Systems pp. 77–84 (2004)
5. Li, G., Svogor, I., Beltrame, G.: Long-term pattern formation and maintenance for battery-powered robots. Swarm Intelligence **13**(1), 21–57 (2019)
6. Liu, M., Yang, F., Michiels, S., Van Eyck, T., Hughes, D., Alvarado-Marin, S., Maksimovic, F., Watteyne, T.: Demo Abstract: FreeBot, a Battery-Free Swarm Robotics Platform. In: The 21st ACM Conference on Embedded Networked Sensor Systems (SenSys '23), November 12–17, 2023, Istanbul, Turkiye (2023)
7. Marques, J.V.A., Lorente, M.T., Groß, R.: Multi-robot systems research: A data-driven trend analysis. In: Distributed Autonomous Robotic Systems. pp. 537–549. Springer Nature Switzerland, Cham (2022)
8. Melhuish, C., Kubo, M.: Collective energy distribution: Maintaining the energy balance in distributed autonomous robots using trophallaxis. In: Distributed Autonomous Robotic Systems 6, pp. 275–284. Springer (2007)
9. Miyauchi, G., Talamali, M.S., Groß, R.: Online supplementary material (2024), `https://doi.org/10.15131/shef.data.25561923`
10. Miyauchi, G., Talamali, M.S., Groß, R.: Robot controller source code. (2024), `https://github.com/genkimiyauchi/swarm-energy-replenishment`
11. Mondada, F., Bonani, M., Raemy, X., Pugh, J., Cianci, C., Klaptocz, A., Magnenat, S., Zufferey, J.C., Floreano, D., Martinoli, A.: The e-puck, a robot designed for education in engineering. Proceedings of the 9th Conference on Autonomous Robot Systems and Competitions **1**(1), 59–65 (2009)
12. Moonjaita, C., Philamore, H., Matsuno, F.: Trophallaxis with predetermined energy threshold for enhanced performance in swarms of scavenger robots. Artificial Life and Robotics **23**(4), 609–617 (2018)
13. Pearson, S., Camacho-Villa, T.C., Valluru, R., Gaju, O., Rai, M.C., Gould, I., Brewer, S., Sklar, E.: Robotics and autonomous systems for net zero agriculture. Current Robotics Reports **3**(2), 57–64 (2022)
14. Pinciroli, C., Trianni, V., O'Grady, R., Pini, G., Brutschy, A., Brambilla, M., Mathews, N., Ferrante, E., Di Caro, G., Ducatelle, F., Birattari, M., Gambardella, L.M., Dorigo, M.: ARGoS: A modular, parallel, multi-engine simulator for multi-robot systems. Swarm Intelligence **6**(4), 271–295 (2012)
15. Pini, G., Brutschy, A., Birattari, M., Dorigo, M.: Interference reduction through task partitioning in a robotic swarm. In: Sixth International Conference on Informatics in Control, Automation and Robotics–ICINCO. pp. 52–59 (2009)
16. Rappaport, M., Bettstetter, C.: Coordinated recharging of mobile robots during exploration. In: 2017 IEEE/RSJ international conference on intelligent robots and systems (IROS). pp. 6809–6816. IEEE (2017)

17. Schioler, H., Ngo, T.D.: Trophallaxis in robotic swarms-beyond energy autonomy. In: 2008 10th International Conference on Control, Automation, Robotics and Vision. pp. 1526–1533. IEEE (2008)
18. Vaussard, F., Rétornaz, P., Roelofsen, S., Bonani, M., Rey, F., Mondada, F.: Towards long-term collective experiments. In: Lee, S., Cho, H., Yoon, K.J., Lee, J. (eds.) Intelligent Autonomous Systems 12. pp. 683–692. Springer Berlin Heidelberg, Berlin, Heidelberg (2013)
19. Warsame, Y., Edelkamp, S., Plaku, E.: Energy-aware multi-goal motion planning guided by monte carlo search. In: 2020 IEEE 16th International Conference on Automation Science and Engineering (CASE). pp. 335–342. IEEE (2020)
20. Winfield, A.F., Kernbach, S., Schmickl, T.: Collective Foraging: Cleaning, Energy Harvesting, and Trophallaxis. In: Handbook of Collective Robotics. Jenny Stanford Publishing (2013)
21. Xie, L., Shi, Y., Hou, Y.T., Lou, A.: Wireless power transfer and applications to sensor networks. IEEE Wireless Communications **20**(4), 140–145 (2013)
22. Yu, K., Budhiraja, A.K., Buebel, S., Tokekar, P.: Algorithms and experiments on routing of unmanned aerial vehicles with mobile recharging stations. Journal of Field Robotics **36**(3), 602–616 (2019)